TAO, Vol.4, No.4, 421-440, December 1993

A Study of High-Order Advection Schemes in Variable Resolution

CHING-YUANG HUANG[1]

(Manuscript received 4 May 1993, in final form 10 December 1993)

ABSTRACT

High-order advection schemes are investigated in linear and nonlinear advection. Numerical tests and theoretical analyses indicate that the performance level of semi-Lagrangian advection schemes using cubic spline interpolation is between those using quintic and seventh-order Lagrange interpolations in uniform resolution. However, higher-order Lagrange interpolations yield larger dispersion in the region of variable resolution in the rotational flow test. The degrading phase preservation can be improved by spline interpolations such as cubic spline or cubic B-spline. For positive definite advection, first-order Lagrange interpolation can be applied in combination with higher-order Lagrange interpolations to suppress the dispersion of negative values. In variable resolution, simple Eulerian formulations generally have insufficient accuracy and stringent stability constraints, but semi-Lagrangian schemes do not. Based on the linear and nonlinear advection tests, it was suggested that variable-resolution mesoscale models may employ cubic spline or cubic B-spline for horizontal advection and cubic Lagrange interpolation for vertical advection without recourse to quintic and higher-order Lagrange interpolations.

1. INTRODUCTION

Semi-Lagrangian advection schemes preserve several important properties of an advective field. These properties include consistency, mass conservation and most important, satisfaction of the shift condition. The last one is a strict requirement for most Eulerian schemes, since the advective field must move downstream by integral grids as directional Courant numbers are integers. For multi-dimensional advection, it is much easier for semi-Lagrangian schemes to obtain this property. An advection scheme that does not satisfy the shift condition will be theoretically deficient, despite that it may perform fairly well in short-term advection.

[1] Department of Atmospheric Sciences, National Central University, Chung-Li, Taiwan 32054, R.O.C.

High-order semi-Lagrangian advection schemes are very accurate in preserving both phase and amplitude in uniform resolution (Pudykiewicz and Staniforth, 1984; Staniforth and Côté, 1991). Furthermore, semi-Lagrangian advection schemes are unconditionally stable (Bates and McDonald, 1982) compared to most of Eulerian advection schemes with the linear stability constraint (i.e., the CFL condition). Although some implicit Eulerian advection schemes are unconditionally stable also, their numerical performances significantly degrade as the chosen Courant number is larger above unity. Unlike Eulerian advection schemes, semi-Lagrangian advection schemes exhibit reasonable accuracy at large Courant numbers. Indeed, the accuracy of semi-Lagrangian advection schemes is only related to the determination of departure points and the properties of the fitting polynomial. Advantages of semi-Lagrangian advection schemes over Eulerian advection schemes have been evidenced by many investigators in the past. For instance, Bermejo (1990) showed that semi-Lagrangian cubic B-spline may well preserve the shape of a slotted cylinder after many revolutions. Kuo and Williams (1990) also presented the excellent performance of semi-Lagrangian cubic spline when applied to evolving flow where a shock point develops.

Semi-Lagrangian advection schemes are more desirable than Eulerian advection schemes for stretched grids, since formulations for the latter become tedious if high-order accuracy remains demanded. Fourth-order Eulerian advection schemes are formally only first-order accurate in non-uniform grids and hence cause appreciable distortion of the solution in the region of varying resolution. In this sense, nesting rather than stretching a numerical model has been overwhelmingly considered. Gravel and Staniforth (1992) have shown that a global model may provide excellent regional forecast when a high-order semi-Lagrangian advection scheme such as bicubic spline is used in stretched grids where resolution is enhanced at regions of interest. In their opinion, a global model is not necessarily nested by a regional model; hence, only one single model needs to be operated, developed and upgraded.

Before we endorse development of a variable-resolution mesoscale model or a nested one, we should investigate the performance of high-order semi-Lagrangian advection schemes in variable resolution. In this study, high-order Lagrange interpolations and splines will be tested in linear and nonlinear advection. In addition to the semi-Lagrangian advection schemes, the fourth-order modified WKL scheme (as a Eulerian advection scheme) proposed in Huang and Raman (1991) will also be tested for comparisons. The paper gives a brief description of the advection schemes in Section 2 followed by the presentation of the numerical results in Sections 3 and 4. Finally, conclusions are given.

2. DESCRIPTIONS OF THE ADVECTION SCHEMES

2.1 The Eulerian WKL Scheme

Huang and Raman (1991) have provided a detailed description of the WKL scheme. The one-step WKL algorithm for the 1-D advection equation is given by

$$\begin{aligned}\phi_i^{n+1} = \phi_i^n &- \frac{\alpha}{12}(-\phi_{i+2}^n + 8\phi_{i+1}^n - 8\phi_{i-1}^n + \phi_{i-2}^n) \\ &+ \frac{\alpha^2}{8}(\phi_{i+2}^n - 2\phi_i^n + \phi_{i-2}^n) \\ &+ \frac{\alpha^3}{12}(-\phi_{i+2}^n + 2\phi_{i+1}^n - 2\phi_{i-1}^n + \phi_{i-2}^n) \\ &- \frac{\omega}{24}(\phi_{i+2}^n - 4\phi_{i+1}^n + 6\phi_i^n - 4\phi_{i-1}^n + \phi_{i-2}^n)\end{aligned} \tag{1}$$

where the directional Courant number $\alpha = u_i \Delta t / h_i$ ($= x_{i+1} - x_i$) for a given time step Δt, and i and n denote the grid index in the x- direction and the nth time level, respectively. This scheme is stable if $|\alpha| \leq 1$ and $4\alpha^2 - \alpha^4 \leq \omega \leq 3$. As discussed in Huang and Raman (1991), this algorithm would yield minimum dissipation with $\omega = \omega_1 = 4\alpha^2 - \alpha^4$ and minimum dispersion with $\omega = \omega_2 = (4\alpha^2 + 1)(4 - \alpha^2)/5 \sim 0.8(4\alpha^2 + 1)$. Hence, the modified WKL algorithm for positive definite scalars may be proposed with

$$\omega = \omega_1 = 4\alpha^2 - \alpha^4 \quad for \quad \phi_i^n > 0, \tag{2a}$$

$$\omega = \omega_2 = 0.8(4\alpha^2 + 1) \quad for \quad \phi_i^n \leq 0, \tag{2b}$$

to allow heavy damping on zero or negative values generated by higher-order schemes. The selective damping is basically a method of flux-corrected transport (FCT) originally proposed by Zalesak (1979). Sun (1993) pointed out that use of ω_2 may lead to WKL scheme's inconsistency because of the unbounded truncation coefficient in Eq. (5) of Huang and Raman (1991). Although we apply ω_2 only in regions of non-positive values (for suppressing such values), the FCT procedure has affected the mass conservation of the WKL scheme in positive definite advection. It should be noted herein that the modified WKL scheme hence is not strictly a positive-definite advection scheme since it does not preserve the sign of each initial grid-point value. Practical test results (Huang and Raman, 1991; Huang, 1993) indicate that local accuracy obtained by the modified WKL scheme remains reasonable, but the increase in total mass is rather large for more complicated flow. The WKL scheme, without the selective damping of (2a) and (2b), is identical to the fourth-order Crowley advection scheme (Crowley, 1968). In 2-D advection, the time-splitting algorithm of the WKL scheme should be used in order to obtain the maximun stability range of x- and y- directional Courant numbers ($|\alpha| \leq 1$ and $|\beta| \leq 1$) and satisfy the shift condition.

2.2 Semi-Lagrangian Cubic Spline

Formulation of cubic spline and its implementation can be found in Pielke (1984). For the jth grid interval h_j, the piecewise cubic spline containing the departure point x_d is given by

$$\begin{aligned} S(x_d) = S(x_i - C^* h_i) = \phi_j^n - CN_j h_j + C^2[N_{j-1}h_j + 2N_j h_j + 3(\phi_{j-1}^n - \phi_j^n)] \\ - C^3[h_j N_{j-1} + h_j N_j + 2(\phi_{j-1}^n - \phi_j^n)] \quad for \quad u_i^n \geq 0 \end{aligned} \tag{3a}$$

$$\begin{aligned} S(x_d) = S(x_i + C^* h_i) = \phi_j^n + CN_j h_{j+1} - C^2[N_{j+1}h_{j+1} + 2N_j h_{j+1} + 3(\phi_j^n \\ - \phi_{j+1}^n)] + C^3[h_{j+1}N_j + h_{j+1}N_{j+1} + 2(\phi_j^n - \phi_{j+1}^n)] \quad for \quad u_i^n < 0 \end{aligned} \tag{3b}$$

where j denotes the jth spline segment where x_d lies on, C^* and C represent the conventional and residual Courant numbers in the x direction, respectively, and N_j to be solved globally is the first-order spatial derivative of the advective field ϕ_j at x_j in the x-direction. For the y-directional advection, the spline formulations are analogous to (3a) and (3b). In

evaluation of the advection change in the y-direction, the updated value after the x-directional advection is used. This time-splitting technique has often been assumed for semi-Lagrangian cubic spline in order to save computation time. Split semi-Lagrangian cubic spline has been successfully applied to simulations of 2-D topographically-induced mesoscale circulations (e.g., Mahrer and Pielke, 1978).

2.3 Lagrange Interpolation

Formulation of Lagrange interpolation is quite straightforward and can be expressed as

$$P_n(x) = \sum_{i=m_1}^{m_2} \prod_{j=m_1}^{m_2} \frac{x - x_j}{x_i - x_j} \phi_i \qquad i \neq j \tag{4}$$

where $n = m_2 - m_1 + 1$ denotes the degree of the polynomial and x is the location of an interpolated point within a span of grid points indexed m_1 to m_2. The grid interpolation is chosen so that the interpolated point, i.e., x, is arrayed as symmetrically as possible in order to reduce biasing of interpolation, which would introduce phase dispersion. As discussed in Purser and Leslie (1988) and shown in Huang (1993), a fitting polynomial used for evaluation of advective change should not be lower than cubics [i.e., $P_3(x)$] for reasonable preservations of both phase and amplitude. It can be easily verified that the second-order Crowley advection scheme and the fourth-order Crowley advection scheme [i.e., Eq. (1)] are the special cases of semi-Lagrangian schemes using $P_2(x)$ and $P_4(x)$, respectively, for uniform flow in uniform resolution. Hence, semi-Lagrangian schemes based on Lagrange interpolation may be specialized into their Eulerian counterparts if a departure point is within the grid cell that involves the arrival grid point. Since semi-Lagrangian advection schemes always employ an interpolation rather than an extrapolation for a departure point, they (based on Lagrange interpolations of any degree and spline interpolations) are unconditionally stable.

One of the major shortcomings for high-order semi-Lagrangian schemes is that they do not formally conserve the total mass that is positive definite. Only the first-order semi-Lagrangian scheme using $P_1(x)$ (whose Eulerian counterpart is the well-known first-order upstream scheme), is a positive-definite scheme that preserves the total mass and also the sign of the initial advective values but at the cost of heavy damping. Similar to the FCT method applied for the modified WKL scheme, semi-Lagrangian schemes for positive definite advection can be modified by using $P_1(x)$ rather than $P_n(x)$ ($n \geq 2$) at regions of zero values surrounding a specific departure point. Such a modified semi-Lagrangian advection scheme, although not strictly positive definite, yields much smaller dispersion of negative values near the boundaries of the advective mass; negative values then are reset to zero. It should be noted that forced positiveness does not distort the phase but would increase the total mass since the negative-value holes are filled up. The modified semi-Lagrangian schemes are also unconditionally stable.

2.4 Determination of Departure Points

Temperton and Staniforth (1987) proposed a two-time-level algorithm for determining departure distance given by

$$\begin{aligned} x' &= \Delta t V(x - x'/2, t + \Delta t/2), \\ V(x, t + \Delta t/2) &= (3/2)V(x,t) - (1/2)V(x, t - \Delta t) + O(\Delta t^2) \end{aligned} \tag{5}$$

where x is the position vector of a grid point and V = dx/dt. This scheme of second-order accuracy requires iterations for solving (5) and needs both temporal and spatial interpolations of departure velocity to obtain departure points. McGregor (1993) proposed a non-iterative scheme instead for saving the computation time. In a terrain-following coordinate system (x, y, σ), the scheme of second order (i.e., the D_2 method) for the coordinate of a departure point (x_d, y_d, σ_d) can be given by

$$\begin{aligned} x_d &= x - \Delta t u + (\Delta t^2/2)(u\frac{\partial u}{\partial x} + v\frac{\partial u}{\partial y} + \tilde{w}\frac{\partial u}{\partial \sigma}), \\ y_d &= y - \Delta t v + (\Delta t^2/2)(u\frac{\partial u}{\partial x} + v\frac{\partial v}{\partial y} + \tilde{w}\frac{\partial v}{\partial s}), \\ \sigma_d &= \sigma - \Delta t \tilde{w} + (\Delta t^2/2)(u\frac{\partial \tilde{w}}{\partial x} + v\frac{\partial \tilde{w}}{\partial y} + \tilde{w}\frac{\partial \tilde{w}}{\partial \sigma}) \end{aligned} \tag{6}$$

where $\tilde{w} = d\sigma/dt$. The D_1 method using only the first-order term in (6) is simplest but does not give enough accurate estimates for departure points in rotational flow when advection calculation is not time-split. For split advection schemes, the D_1 method may also obtain good accuracy, particularly for smaller Courant numbers. McGregor (1993) showed that the D_2 method used in combined advection schemes may obtain acceptable accuracy for non-divergent flow.

2.5 The Lateral Boundary Condition

The lateral boundary condition used in this study is a radiation condition,

$$\begin{aligned} \phi_b^{n+1} &= \phi_b^n - r(\phi_b^n - \phi_{b1}^n), and \\ r &= (\phi_{b1}^{n+1} - \phi_{b1}^n)/(\phi_{b2}^n - \phi_{b1}^n) \quad for \quad 0 \le r \le 1, \end{aligned} \tag{7}$$

where subscripts b, $b1$, and $b2$ indicate a boundary grid point, and the first and second grid points adjacent to the boundary, respectively.

3. THE LINEAR ADVECTION TESTS

3.1 Designs of Linear Advection Tests

The linear advection tests are based on 2-D uniform flow (UL) and rotational flow (RL) that have been found to well present the characteristic features of a scheme. A uniform grid interval h_i of 5 km is set from i = 1 to i = 20 and i = 60 to i = 79 and in between a smaller grid interval of 1 km is used. To avoid the effects of a sharp change in grid resolution, linearly varying grid intervals (grids 21 to 24 and 56 to 59) have been used between the coarse mesh and the fine mesh. This grid arrangement is also applied to the y-direction. Hence, there is a uniform fine grid mesh in the central domain as seen in Figure 1.

The tested advective fields contain two cosine cones described by a 2-D function,

$$\phi_{i,j} = \begin{cases} 50[1 + cos(\frac{\pi R_{i,j}}{k\Delta})], R_{i,j} \le k\Delta \\ 0, \qquad\qquad\qquad R_{i,j} > k\Delta \end{cases} \tag{8}$$

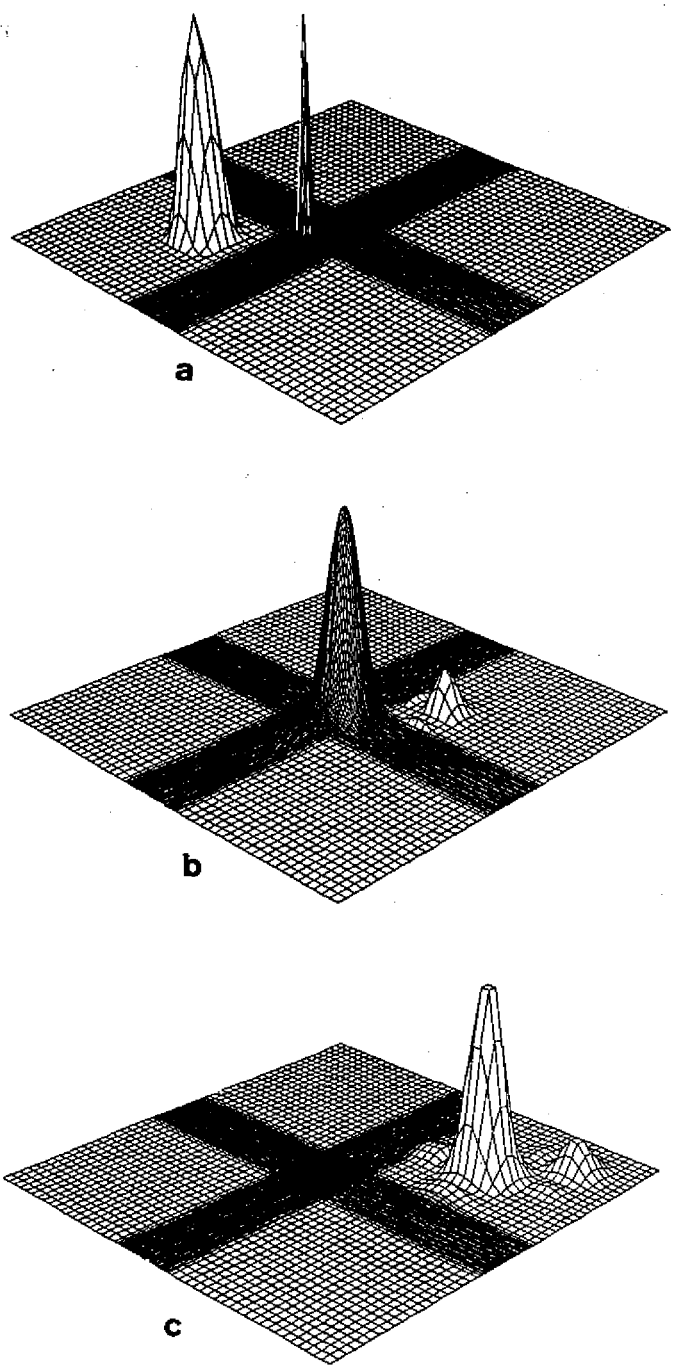

Fig. 1. The positive-definite advective field in the uniform-flow test using the split modified WKL scheme with a time step of 60 s. (a) at 0 h (the original cones); (b) at 3 h; (c) at 6 h.

where

$$R_{i,j} = [(x_i - x_p)^2 + (y_j - y_p)^2]^{1/2}$$

for a given cone peak at (x_p , y_p) and Δ indicates a coarse or fine grid interval with grid indices i in x and j in y.

The wind velocity components $U_{i,j}$ (in the x-direction) and $V_{i,j}$ (in the y-direction) are 5 m s^{-1} in the UL test, and

$$U_{i,j} = -(y_j - y_c)\Omega, \quad V_{i,j} = (x_i - x_c)\Omega \tag{9}$$

in the RL test where (x_c, y_c) = (40, 40) is chosen as the center of the rotation. In the RL test, the initial field will complete one full revolution per four hours with the specified angular velocity Ω.

3.2 Properties of the Tested Schemes

As mentioned before, some semi-Lagrangian advection schemes using low-order Lagrange interpolations in fact are general representations of their well-known Eulerian counterparts which have been widely discussed in the literature. Tremback *et al.* (1987) have discussed the stabilities and performances of the forward-in-time upstream advection schemes up to tenth-order based on Lagrange interpolations. Since the interpolation algorithm in semi-Lagrangian sense is identical to the Eulerian one, the Eulerian analyses remain valid for the equivalent semi-Lagrangian schemes provided that the residual Courant number is the same. Based on Fourier component analyses, Table 1 shows amplification factors and phase speed ratios for 4-Δx waves for Lagrange interpolations from first order (LA1) to eighth order (LA8) and cubic spline (CSP). We should herein clarify some points and state the important information:

(1) For 2-Δx waves, all the schemes fail to preserve good amplitude and phase except when the Courant number is unity. For 8-Δx waves, even the second-order scheme loses only 0.1% of amplitude. The preserved amplitude for the fourth- and higher- order Lagrange interpolations and cubic spline are better (with lose to the fourth decimal) for 8-Δx waves and longer waves.

(2) All the schemes of odd order show minimum dispersion and maximum dissipation at the Courant number of 0.5 since they are formulated symmetrically about the departure point. For even-order schemes, the dispersion gradually vanishes toward the Courant number of unity because of the more symmetrical interpolation and the dissipation is larger as the Courant number is smaller.

(3) LA4 (quartic) exhibits better amplitude preservation than LA3 (cubic) but produces larger dispersion of lagging that is similarly exhibited by the fourth-order leapfrog scheme. Both phase and amplitude are reasonably preserved by LA4 even at the Courant number of 0.01; hence no inconsistency is observed for the equivalent WKL scheme since selective damping is not employed.

(4) LA5 (quintic) preserves similar amplitude as for LA4 but has improved the phase speed ratio. LA6 further increases the amplitude preservation of LA5 but at the cost of worse phase preservation (which is still better than for LA4).

(5) LA7 enhances the phase preservation of LA6 but retains the ability of LA6 in amplitude preservation. Similarly, LA8 increases the preserved amplitude of LA7 but slightly degrades phase preservation.

Table 1. Amplification factor and phase speed ratio (between the numerical one and the analytical one) for 4-Δx waves at different Courant numbers for Lagrange interpolations from first-order (LA1) to eighth-order (LA8) and cubic spline (CSP).

Schemes	0.01	0.1	0.3	0.5	0.7	0.9	1.0
			Amplification factor				
LA1	0.990	0.906	0.762	0.707	0.762	0.906	1.000
LA2	1.000	0.995	0.958	0.901	0.866	0.920	1.000
LA3	0.997	0.966	0.908	0.884	0.908	0.966	1.000
LA4	1.000	0.997	0.978	0.952	0.943	0.971	1.000
LA5	0.999	0.986	0.961	0.950	0.961	0.986	1.000
LA6	1.000	0.999	0.989	0.978	0.975	0.988	1.000
LA7	0.999	0.994	0.983	0.978	0.983	0.994	1.000
LA8	1.000	0.999	0.995	0.990	0.989	0.995	1.000
CSP	1.000	0.997	0.981	0.972	0.981	0.997	1.000
			Phase speed ratio				
LA1	0.643	0.704	0.859	1.000	1.060	1.033	1.000
LA2	0.637	0.641	0.676	0.749	0.856	0.964	1.000
LA3	0.852	0.879	0.945	1.000	1.023	1.013	1.000
LA4	0.849	0.852	0.873	0.911	0.956	0.991	1.000
LA5	0.935	0.947	0.976	1.000	1.010	1.006	1.000
LA6	0.934	0.935	0.946	0.964	0.983	0.997	1.000
LA7	0.971	0.976	0.989	1.000	1.005	1.003	1.000
LA8	0.970	0.971	0.976	0.984	0.993	0.999	1.000
CSP	0.955	0.958	0.979	1.000	1.009	1.005	1.000

(6) For 4-Δx waves, cubic spline (CSP) preserves amplitude better than LA5, comparably to LA6 and LA7, but worse than LA8. The preserved phase for CSP is slightly worse than for LA7 but better than for LA6.

3.3 Linear Advection in Uniform Resolution

Before discussing the performances of the schemes in variable resolution, we should present their results in uniform-resolution tests. Uniform advection and rotation tests are chosen to compare LA3, LA5, LA7 and CSP. For both the tests, an initial cone is located on (20, 20) and moves diagonally in the uniform-advection test or around the rotation center of (40, 40) in the rotation test. Table 2 lists three performance indices for the four schemes. All the semi-Lagrangian schemes in both the tests exhibit excellent mass conservation (more than 99.5% of the total masses defined by sum of all grid-point values); also, the cone peak returns to the initial position for all the schemes after one full revolution.

The test results show that cubic Lagrange interpolation obtains excellent phase, but the amplitude could lose more than one-half in both tests when Courant numbers are smaller. Since numerical dissipation and dispersion are functions of Courant number and operation time, the exact preservation is not as simple as one can intuitively estimate. For instance, in the uniform-advection test the results using Δt of 960 s (thus $\alpha = \beta = 0.96$) are better than

Table 2. Performance indices* of selected schemes for a cone with 4-Δx half-width in uniform resolution. The time step Δt of 60 s corresponds to a uniform Courant number of 0.06 in the uniform flow test and the maximum directional Courant number α and β of 1.048 in the rotational flow test.

	LA3	LA5	LA7	CSP
		After 12 hours of uniform advection		
Δt=30 s	(48.9, -4.2, 53.6)	(81.2, -6.0, 85.8)	(94.5, -3.0, 95.9)	(95.9, -6.8, 97.0)
Δt=60 s	(49.2, -4.1, 53.9)	(81.3, -5.9, 85.8)	(94.5, -3.0, 95.9)	(93.7, -5.7, 94.7)
Δt=120 s	(49.9, -3.9, 54.5)	(81.6, -5.7, 86.0)	(94.5, -3.0, 95.9)	(90.5, -4.6, 91.4)
Δt=240 s	(51.8, -3.5, 56.2)	(82.4, -5.1, 86.7)	(94.8, -3.1, 96.1)	(87.1, -4.1, 88.1)
Δt=360 s	(54.3, -3.4, 58.6)	(83.7, -4.6, 87.7)	(95.2, -3.0, 96.4)	(86.3, -3.5, 87.5)
Δt=480 s	(57.6, -3.3, 61.9)	(85.6, -4.0, 89.1)	(96.0, -2.9, 96.9)	(87.4, -2.8., 88.6)
Δt=960 s	(93.8, -2.2, 93.9)	(98.6, -1.4, 98.9)	(99.1, -0.9, 99.7)	(98.5, -1.0, 99.8)
Δt=1800 s	(86.2, -2.8, 87.3)	(97.3, -2.3, 97.4)	(99.5, -1.5, 99.3)	(98.4, -1.7, 98.3)
		After one full rotation (4 hours)		
Δt=5 s	(34.4, -2.3, 39.0)	(68.6, -4.8, 76.1)	(87.6, -4.5, 91.8)	(80.7, -9.9, 90.2)
Δt=10 s	(34.8, -2.2, 39.5)	(68.9, -4.7, 76.3)	(87.8, -4.4, 91.9)	(78.2, -7.4, 85.1)
Δt=15 s	(35.3, -2.0, 39.9)	(69.3, -4.5, 76.6)	(88.0, -4.2, 92.0)	(76.4, -5.9, 81.9)
Δt=30 s	(37.4, -2.1, 42.0)	(71.1, -4.0, 77.9)	(89.1, -3.7, 92.5)	(74.4, -3.6, 78.0)
Δt=60 s	(44.9, -2.0, 49.5)	(77.4, -3.2, 82.7)	(92.8, -2.8, 94.5)	(80.5, -2.5, 82.6)
Δt=120 s	(59.1, -2.2, 62.8)	(87.0, -2.8, 89.5)	(97.5, -2.0, 97.0)	(90.7, -2.3, 90.4)
Δt=240 s	(72.8, -1.8, 74.9)	(93.7, -2.0, 94.0)	(99.9, -1.4, 98.4)	(96.4, -1.4, 95.1)
Δt=360 s	(79.8, -1.7, 80.7)	(96.0, -1.8, 95.6)	(100., -1.3, 98.8)	(97.7, -1.2, 96.6)

*The indices are chosen as [max of $\phi^n_{i,j}$, min of $\phi^n_{i,j}$, $\sum\sum(\phi^n_{i,j})^2 / \sum\sum(\phi^0_{i,j})^2$]. The former two indices are in absolute units and the last index is in percentages. Total mass (sum of all the grid-point values) is not given herein since it is about 100 % preserved for all runs.

that using 1800 s ($\alpha = \beta = 1.8$) because the interpolation point for the former is closer to the grid point. Fortunately, more operations do not cause further reduction in amplitude and accumulate phase errors. These results may support the use of the famous LA3 in meteorological modeling.

The semi-Lagrangian schemes going to higher odd orders (LA5 and LA7) significantly improve the amplitude for LA3 without sacrificing phase preservation. On the other hand, the even-order scheme of LA4 obtains similar amplitudes for LA5 but exhibits much worse phase (with negative values smaller than -10). Hence, the uniform-resolution test results may recommend the quintic form rather than the quartic form. In general, LA7 shows the best performance of phase and amplitude in both uniform-advection and rotation tests for various Courant numbers as theoretically indicated in Table 1. The performance of LA6 (not shown) is similar to LA7 in amplitude but with increased phase dispersion that is also evident in Tremback *et al.* (1987). Tremback *et al.* (1987) suggested the sixth-order scheme (LA6) as the optimum between accuracy and efficiency. But, our numerical results seem to imply that higher-order interpolation than sixth-order should be deserved. The superiority of LA8 to LA6 has also been evidenced by the results of 100 case forecasts (Purser and Leslie, 1993).

According to Table 1, LA8 further improves the amplitude for LA7 but would degrade the phase preservation. Also, the coding efficiency (such as vectorization) of LA8 in a semi-Lagrangian sense decreases since even-order schemes have to judge a less biased interpolation as LA2 clearly demonstrates (in an Eulerian sense, the even-order schemes would be more efficient because of the counted arrival point as centrally surrounded by the interpolation points). We therefore prefer the use of LA7 for the semi-Lagrangian algorithms.

The performance of CSP is particularly interesting since its formulation relies on a smooth spline of each piecewise cubic polynomial. As seen in Table 2, CSP becomes more competitive to LA7 when operation times are less, but its dispersion errors tend to accumulate around the cone for very small Courant numbers. Both theoretical results and the practical test results suggest that CSP would give about the accuracy of LA6 in preserving 4-Δx waves. Hence, both phase and amplitude preserved by CSP are better than by LA5, except at very small Courant numbers.

Higher-order advection schemes would obtain better amplitude for longer waves. For example, the fourth-order WKL scheme was found to preserve slightly higher amplitude than CSP in a rotation test in which a cone of 8-Δx half width undergoes two full revolutions (Huang, 1993). In practice, all semi-Lagrangian advection schemes higher than cubics exhibit better amplitude than CSP because the order of interpolating polynomials is higher than cubic. However, the computation time for the Lagrange interpolation schemes higher than quartic is more expensive than CSP; herein, vectorization and special coding efficiency for Lagrange interpolations as discussed in Purser and Leslie (1991) are not counted. When the quartic semi-Lagrangian scheme is specialized into the Eulerian form (i.e., the WKL scheme), it is faster than CSP.

3.4 Linear Advection in Variable Resolution

The previous subsection has shown the basic properties and the practical performances of the advection schemes in uniform resolution. These advection schemes need to be more thoroughly tested in variable resolution as used in a stretched-grid model. As in the uniform-resolution tests, same uniform advection and rotation are chosen but in variable resolution. Initially, the coarse cone peak is specified at grid (15, 15) and the fine cone peak at grid (30, 30), both with $k = 4$. The two cones have the initial maximum height of 100 units as described in Section 2a.

The two-time-level fourth-order WKL scheme produces remarkable dispersion close to that obtained by the three-time-level fourth-order leapfrog scheme. The modified WKL scheme for positive-definite advection remains fourth-order accurate without causing large dispersion in rotational flow tests (Huang and Raman, 1991). Huang (1993), however, found that in severe deformational flow tests the modified WKL exhibits much less acceptable mass conservation but is still better than that for the second-order leapfrog scheme and the Crowley scheme. This time-saving scheme thus deserves further investigation in the variable-resolution tests in which its local accuracy might be largely reduced. Figure 1 shows the UL test results at 3 h and 6 h for this scheme with a time step of 60 s (maximum $\alpha = \beta = 0.3$). At 3 h, the coarse cone has entered the fine mesh and is well represented by the fine grid-spacing there. The reconstructed cone is very similar to the original cone in width and height, but is associated with visible dispersion of positive values. The initial fine cone moves downstream to the coarse mesh and has been lowered and significantly broadened in order to approximately preserve the total mass. When the reconstructed cone also moves to

the downstream coarse mesh, little distortion is caused, however. The modified fourth-order WKL scheme, despite degrading to be formally first-order accurate in variable resolution, exhibits acceptable results when the cone has moved to uniform grids.

The WKL scheme is a special case of semi-Lagrangian schemes using quartic Lagrange interpolation under uniform flow and grids; hence both the Eulerian and semi-Lagrangian schemes perform identically. Although quartic interpolation preserves amplitude better than cubic interpolation, it is earned at the cost of worse phase preservation. To remedy the phase dispersion caused by fourth-order interpolation, an interpolation of higher odd order (e.g., a quintic form) may be in demand. For positive definite advection, the dispersion errors of negative values can be further reduced by the FCT method as discussed before.

Figure 2 shows the results using the same time step (60 s) for the modified quintic interpolation scheme employing the selective damping of $P_1(x)$. As seen, the dispersion for the modified WKL scheme in Figure 1 has been suppressed by the selective damping of the quintic scheme and the maximum amplitude remains equally preserved. Although the modi-

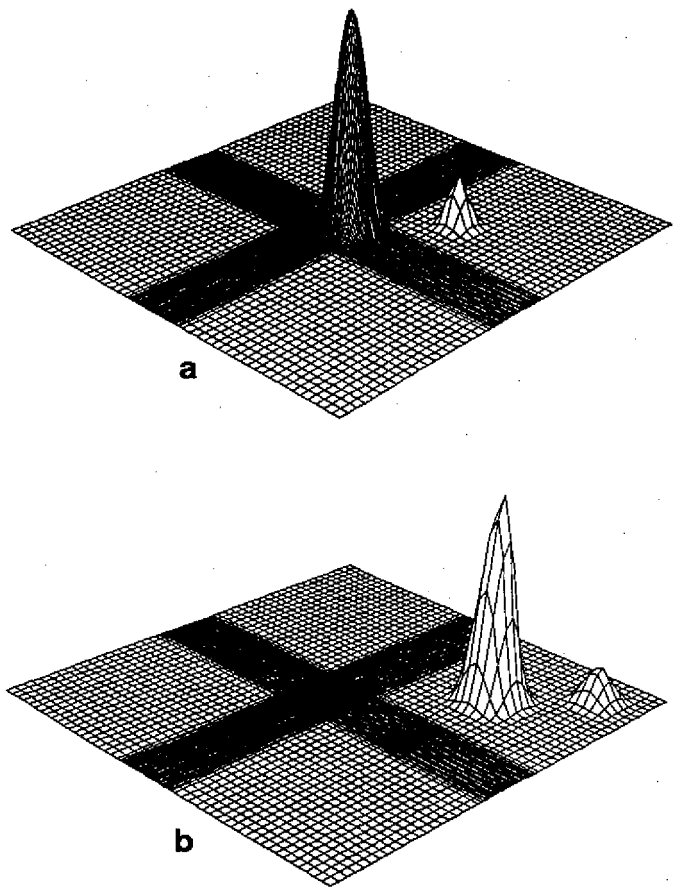

Fig. 2. The positive-definite advective field in the uniform-flow test using the modified quintic Lagrange interpolation with a time step of 360 s. (a) at 3 h; (b) at 6 h.

fied WKL scheme also employs selective damping, its larger inherent dispersion of positive values cannot be removed by FCT. Because of the excellent inherent phase preservation (also evident in Tables 1 and 2), quintic Lagrange interpolation performs very well in the uniform-advection test with variable resolution. This is largely due to the fact that dispersion errors would not accumulate for uniform flow.

Lagrange interpolation schemes are theoretically known to perform more poorly in stretched grids since $P_n(x)$ must satisfy the n interpolating grid-point values and hence causes more oscillations within sparse grids if n is larger. This feature may be improved by cubic spline interpolation that enforces a "global" smooth curve for all grid-point values. Since cubic spline interpolation within a grid interval is always cubic, no large oscillation will be likely to occur even within two sparse grids. The fact is evident in Figure 3 showing the RL test results for quintic interpolation and cubic spline interpolation using Δt of 60 s (maximum α and β equal to 3.3). The numerical results were obtained using the D_1 method to determine departure points for these two split semi-Lagrangian advection schemes. Light dispersion in the varying resolution zone has resulted after one full revolution for the modified quintic interpolation (note that the prominent dispersion is significantly suppressed in the uniform-resolution test); also, the maximum amplitude of the coarse cone is less than 90. In the cases with both α and β smaller than one, the preserved amplitude for the modified WKL scheme and the modified quintic interpolation is very similar. As expected, cubic spline preserves excellent amplitude and phase (both coarse and fine cone peaks return to their original locations exactly after one full revolution). The results also indicate that resetting negative values to zero limits the undershooting of cubic spline but causes no adverse effects on phase preservation. Selective damping (as applied in quintic Lagrange interpolation) is also tested for cubic spline, but it does not produce any difference.

For scalars without positive definiteness, quintic Lagrange interpolation obtains remarkable dispersion around the fine cone. The dispersion has reached the coarse mesh after one full revolution as shown in Figure 4 (the dispersion is confined around the cone in the uniform-resolution tests, however). The spreading dispersion can be effectively reduced by using a wider adjustment zone between the two grid meshes or simply putting the fine cone away from the boundary of the fine mesh. Or alternatively, one may employ more effective semi-Lagrangian advection schemes using cubic spline or cubic B-spline. Cubic B-spline herein employs tensor products and it is locally representative of bicubic spline (see Bermejo, 1990); for regular grids, both cubic B-spline and bicubic spline are mathematically equivalent. Theoretical departure points (derived analytically) are used for the cubic B-spline run in the rotation test. As seen from Figure 4, spline interpolations obtain much better phase for advection in variable resolution. To further compare the performances of higher-order Lagrange interpolations and spline interpolations, the same experiments with various Courant numbers have been conducted. Figure 5 shows the values of the fine cone peak and the minimum grid-point values for LA5, LA7 and CSP using different time steps. As can be clearly seen, the peak of the fine cone is best preserved by LA7. However, the phase for LA7 is worst among the schemes, with the locally confined maximum negative amplitude below -30. The strong dispersion for LA7 in the rotation test with variable resolution may deduct its advantage of amplitude preservation. As expected, CSP obtains the best phase. For this case, the results for cubic B-spline (not drawn in the figure) are almost identical to those for CSP and have justified the use of split semi-Lagrangian cubic spline interpolation in 2-D advection. Finally, the scalar conservation in variable resolution should be discussed.

It was found that even the spline runs do not well preserve the sum of all the grid-point values (e.g., loss is more than one-third of the total mass) as the major mass is passing over

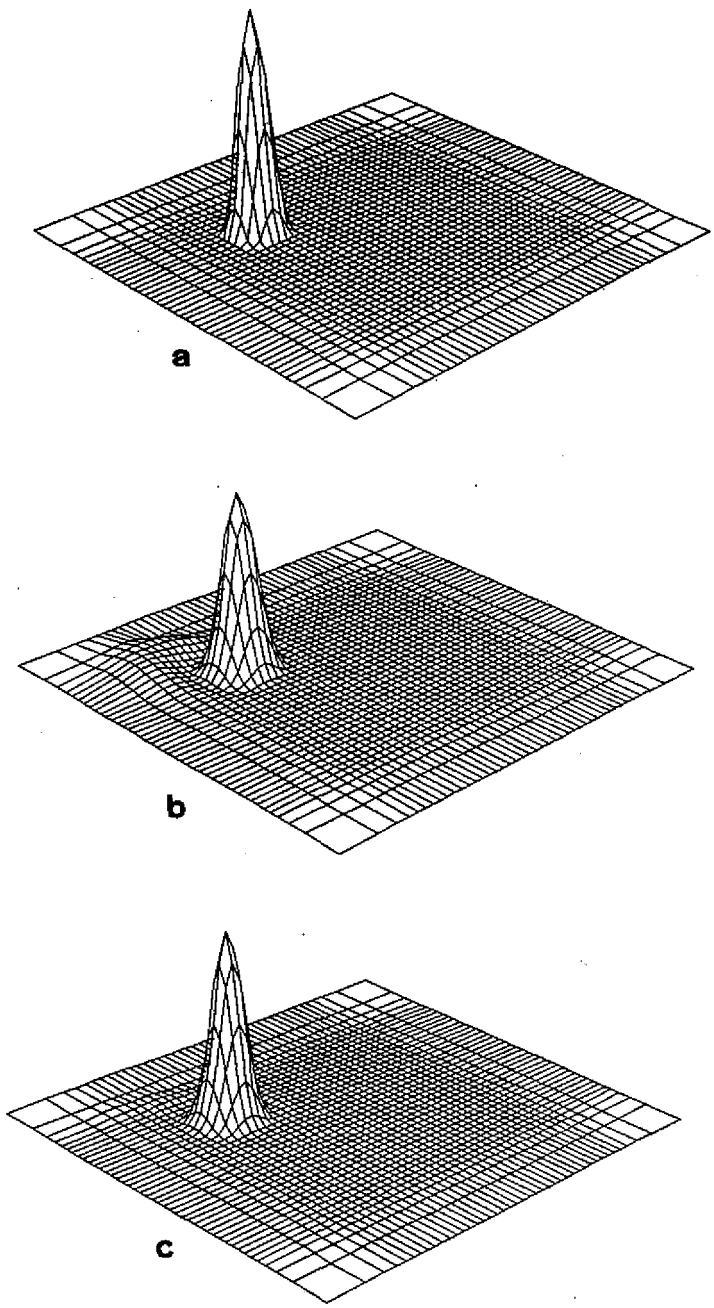

Fig. 3. The positive-definite advective field in the fine mesh. (a) the original cone; (b) after one full revolution for the modified quintic Lagrange interpolation; and (c) after one full revolution for cubic spline.

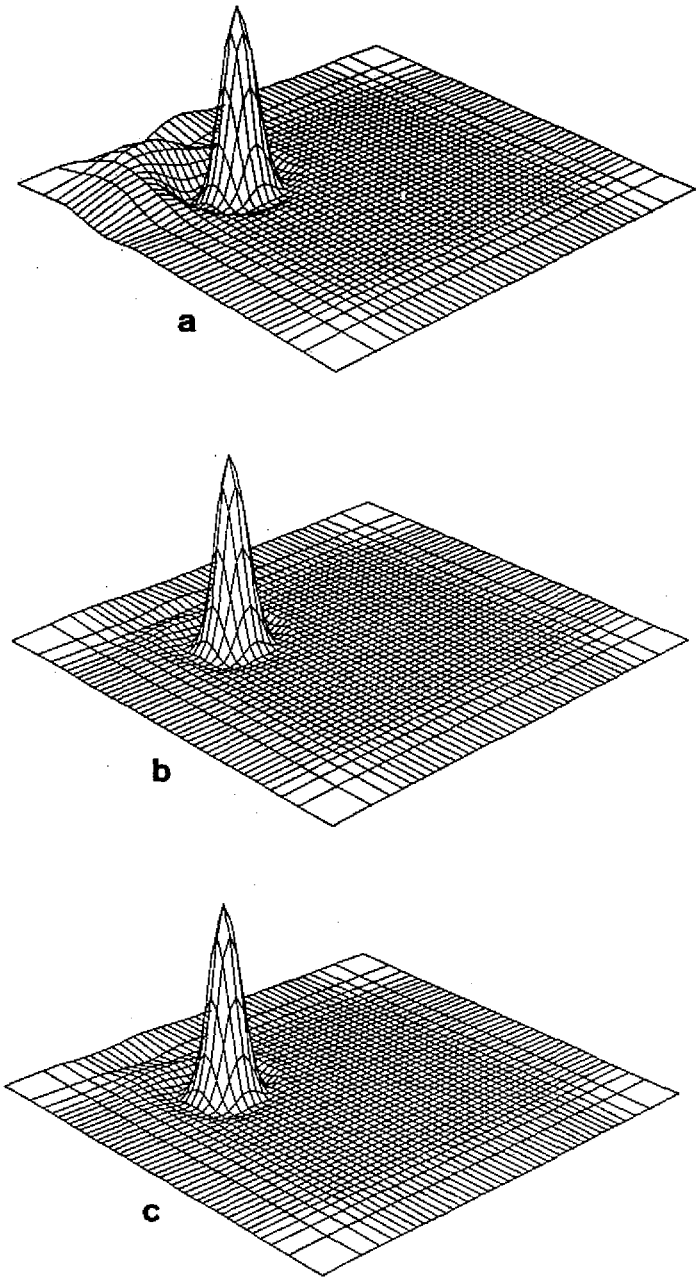

Fig. 4. The advective field without positive definiteness after one full revolution in the fine mesh. The results are obtained using a time step of 60 s for (a) quintic Lagrange interpolation; (b) cubic spline; and (c) cubic B-spline.

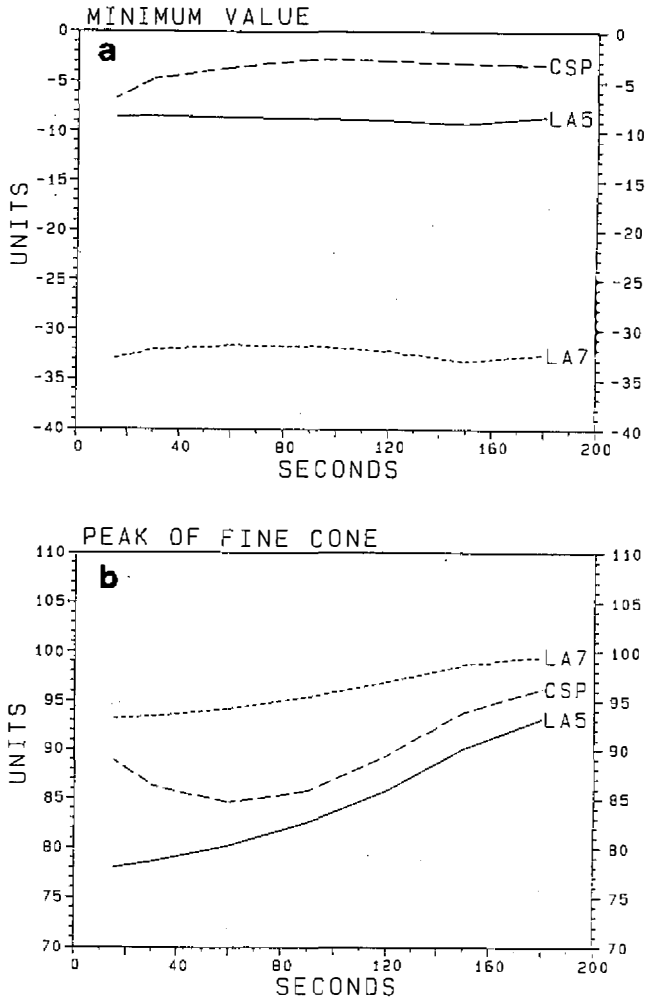

Fig. 5. The numerical results as a function of time steps for LA5 (quintic Lagrange interpolation), LA7 (seventh-order Lagrange interpolation) and cubic spline after one full revolution. (a) the minimum values of the advective field; (b) the magnitude of the fine cone peak. For Δt of 60 s, the corresponding directional Courant numbers (α and β) are 0.26 on the grid of the fine cone peak, and the domain maximum values of α and β are 3.31.

the stretched grids. Transient mass conservation is not reported herein because over stretched grids the integrated form of the grid-point values should be used for the total mass and is more subject to large truncation errors. More important, the cone during the transition stage is also reshaped in some complicated ways so that it may evolve into the initial shape as it returns to constant grids. This property of the spline performance in variable resolution should be further investigated by more complex situations where various forcings may exist.

4. THE NONLINEAR ADVECTION TEST

We choose the simulation of inviscid mountain waves as the nonlinear advection test, since the structure of mountain flow with a given Froude number is well known from linear theory. No boundary-layer mixing is assumed in this test and the initial ambient flow is uniform and westerly at a speed of 20 m s^{-1}. The horizontal grids are also uniform with Δx of 10 km. The vertical grid spacing may be rather irregular depending on cases. The irregularity is made by inserting three additional levels of 50, 8020, and 8040 m, into uniform grid levels at an interval of 500 m (due to these three levels, the maximum vertical Courant number is larger than unity)

We have used Eq. (5) to determine departure points for advection at the level of 50 m and Eq. (6) above this level. By assuming that the flow is stationary within the order of Δt, we did not employ temporal interpolation for the departure velocity. Since the Courant number used is rather small, the departure point can almost be exactly determined. Figure 6 shows the simulated results of near-steady state at 12 h using cubic spline in the horizontal advection and cubic Lagrange interpolation in the vertical; no numerical smoothing has been employed in the run. It is clearly seen from this figure that the inviscid nonlinear mountain waves are excellently reproduced by the advection schemes without causing detectable phase errors. In this case, uses of Crowley advection schemes lead to numerical instability unless

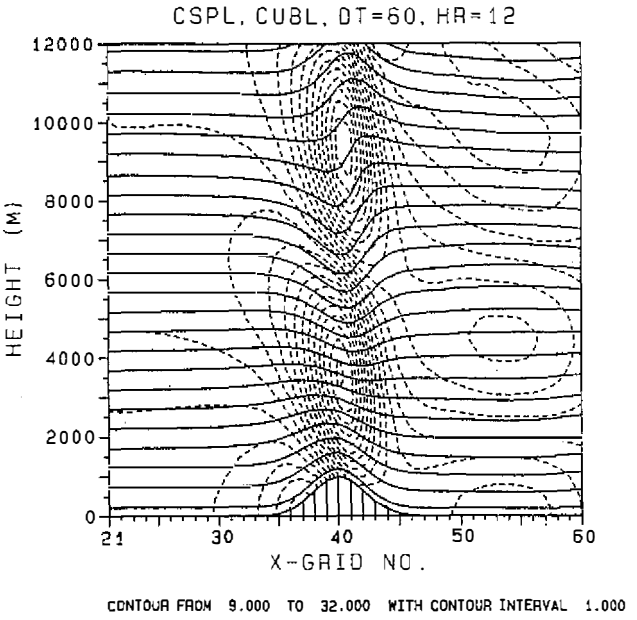

Fig. 6. The numerical results at 12 h in the simulation of inviscid nonlinear mountain waves using cubic spline for horizontal advection and cubic interpolation for vertical advection; a time step of 60 s is used in this case. Froude number of the simulated flow is 2.0 initially.

the three additional levels are removed. We also tested vertical quadratic Lagrange interpolation and found that the mountain waves from this test are almost identical to those for cubic Lagrange interpolation, except that the upstream wind field exhibits very weak dispersion below 8 km (not shown). This dispersion is not present, however, when the upper two of the three fine layers are not inserted. Figure 7 shows the results at 12 h using horizontal cubic spline and vertical second-order Crowley advection scheme in the same experiment but with the no-slip boundary condition (the upper two fine grid intervals were removed in this test); Shapiro's shortwave filter is not employed in this test. Compared to Figure 6, the mountain waves obtained using the second-order Eulerian scheme are slightly weaker than those using cubic Lagrange interpolation, but their preserved phases are equivalently good.

With the no-slip boundary condition, the simulated flow obtained using fully semi-Lagrangian algorithms turns out to be distorted near the lowest boundary (not shown). We have tested a much smaller time step but it does not cure the solution of this problem. One may wonder why the Eulerian one (second-order Crowley scheme) is capable of yielding the feasible solution as shown in Figure 7 but the Lagrangian one is not. We found that second-order Eulerian schemes significantly underestimate the wind shear within the lowest layer and the Eulerian solution is similar to that with the free-slip condition. The flow also becomes distorted near the lowest boundary when the first-order upstream scheme (its truncation error is not biased by adjacent stretched grids) is used instead near the boundary. Due to the accurate evaluation of advection in presence of a large wind shear near the surface, semi-

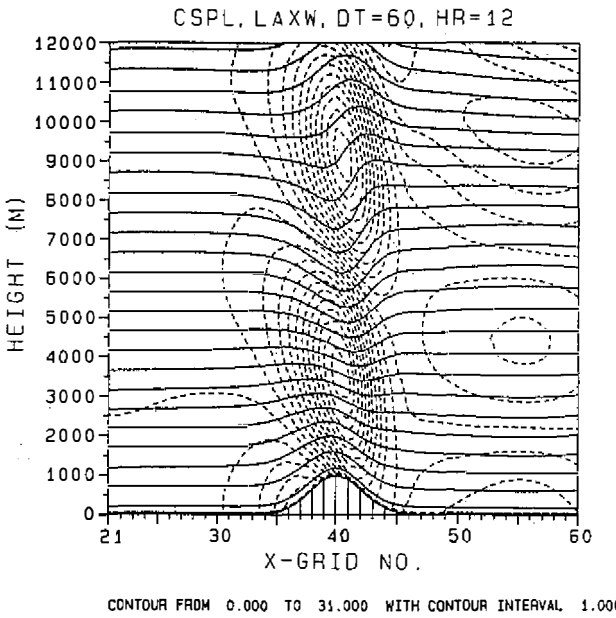

Fig. 7. The numerical results at 12 h in the simulation of nonlinear mountain waves using cubic spline for horizontal advection and second-order Crowley scheme for vertical advection; a time step of 60 s is used in this case. A no-slip lower boundary condition is imposed for the simulated flow with Froude number of 2.0 initially.

Lagrangian advection schemes produce distorted mountain flow near-surface. Physically, the mountain flow near the surface should become turbulent in this case since its Richardson number is less than the critical value (0.25), and under such a condition vertical mixing would take place to adjust the solution.

Although semi-Lagrangian schemes are unconditionally stable when integrating advection modes, a mesoscale anelastic model using such schemes is also subject to stability of gravity-wave modes. For example, the explicit forward-backward scheme for the 2-D shallow water equations (which uses the new values of the momentum fields to compute advection of the fluid surface height) will be stable if $(gH)^{1/2}\Delta t/2\Delta x \leq 1$ (where g is gravity acceleration and H is the shallow water height). The influence of gravity waves on numerical instability can be ruled out in the simulation of neutral mountain flow. Figure 8 shows the results of such an experiment at 100 h using a semi-Lagrangian advection scheme with a time step of 1800 s. As seen, the neutral flow exhibits uniform vertical motions in the vertical. The results are almost identical to theoretical prediction. Apparently, the semi-implicit integration of gravity-wave modes should be incorporated into a mesoscale model in order to have the advantage at use of larger stable Courant numbers for semi-Lagrangian advection schemes. It has been shown that semi-implicit semi-Lagrangian models can use Courant numbers that are an order larger than the maximum one for Eulerian models without causing instability and degrading the solution noticeably (Staniforth and Côté, 1991).

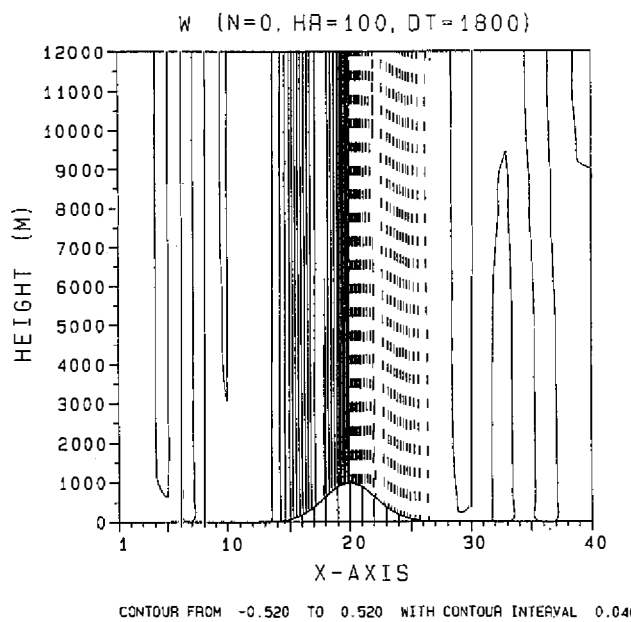

Fig. 8. The numerical results at 100 h in the simulation of nonlinear neutral mountain flow using a time step of 1800 s. Initially, the flow is uniform and westerly at a speed of 20 m s^{-1}. Advection schemes used in this case are the same as in Fig. 6.

5. CONCLUSIONS

We have tested high-order advection schemes in both linear and nonlinear flow tests. The advection schemes tested include the Eulerian WKL scheme and semi-Lagrangian schemes. It was found that semi-Lagrangian schemes using fifth-order (quintic) Lagrange interpolation may preserve amplitude and phase comparable to those using cubic spline interpolation. Seventh-order Lagrange interpolation does perform better than cubic spline and cubic B-spline in the uniform-resolution tests. Both quintic and seventh-order Lagrange interpolations, however, produce remarkable dispersion of negative values in the variable-resolution tests; the large dispersion errors for seventh-order Lagrange interpolation have underquoted its excellent amplitude preservation. In order to reduce the dispersion of negative values, selective damping using first-order Lagrange interpolation can be applied in combination with higher-order Lagrange interpolations. For positive definite advection, such modified Lagrange interpolations of fourth order and higher orders performs better phase without sacrificing amplitude, but usually at the cost of an increase in total mass. In variable resolution, spline interpolations (such as cubic spline and cubic B-spline) are much better than Lagrange interpolations in preserving phase. Both cubic B-spline and bicubic spline are very expensive since their computation operations are theoretically one order larger than those for split cubic spline. Because of the unsplit algorithm, cubic B-spline (or bicubic spline) would preserve better phase than split cubic spline in long-term advection tests when Courant numbers far exceed unity.

Although the WKL scheme (as a specialized scheme of quartic Lagrange interpolation) is competitive to quintic Lagrange interpolation in amplitude preservation, the former scheme exhibits considerably worse phase in various tests. The split Eulerian treatment for advection also suffers from the CFL stability condition where each directional Courant number cannot exceed one. Since semi-Lagrangian advection schemes are unconditionally stable, use of fine resolution does not influence their numerical stabilities. In mountain wave simulations with sharply varying vertical resolution, the combination of horizontal cubic spline and vertical cubic Lagrange interpolation reproduces the theoretical results without causing detectable phase dispersion. Variable-resolution mesoscale models may employ semi-Lagrangian advection schemes where spline interpolations (e.g., cubic spline or cubic B-spline) are used for horizontal advection and cubic Lagrange interpolation for vertical advection.

Acknowledgments Computational support of the VAX 9320 computer by the Computer Center of National Central University is appreciated. Suggestions from one of the reviewers were also helpful in completing this work.

REFERENCES

Bates, J. R., and A. McDonald, 1982: Multiply-upstream, semi-Lagrangian advective schemes: Analysis and Application to a multi-level primitive equation model. *Mon. Wea. Rev.*, **110**, 1831-1842.

Bermejo, R., 1990: On the equivalence of semi-Lagrangian schemes and particle-in-cell finite element method. *Mon. Wea. Rev.*, **118**, 979-987.

Crowley, W. P., 1968: Numerical advection experiments. *Mon. Wea. Rev.*, **96**, 1-11.

Gravel, S., and A. Staniforth, 1992: Variable resolution and robustness. *Mon. Wea. Rev.*, **120**, 2633-2640.

Huang, C. Y., and S. Raman, 1991: A comparative study of numerical advection schemes featuring a one-step WKL algorithms. *Mon. Wea. Rev.*, **119**, 2900-2918.

Huang, C. Y., 1993: A note on semi-Lagrangian schemes and Eulerian WKL algorithms. *Mon. Wea. Rev.*, in press.

Kuo, H.-C., and R. T. Williams, 1990: Semi-Lagrangian solutions to the inviscid Burgers equation. *Mon. Wea. Rev.*, **118**, 1278-1288.

Mahrer, Y., and R. A. Pielke, 1978: A test of an upstream spline interpolation technique for the advection terms in a numerical mesoscale model. *Mon. Wea. Rev.*, **106**, 818-830.

McGregor, J. L., 1993: Economical determination of departure points for semi-Lagrangian models. *Mon. Wea. Rev.*, **121**, 221-230.

Pielke, R. A., 1984: Mesoscale Meteorological Modeling. Academic Press, 612 pp.

Pudykiewicz, J., and A. Staniforth, 1984: Some properties and comparative performance of the semi-Lagrangian method of Robert in the solution of the advection-diffusion equation. *Atmos.-Ocean*, **22**, 283-308.

Purser, R. J., and L. M. Leslie, 1988: A semi-implicit semi-Lagrangian finite-difference scheme using high-order spatial differencing on a nonstaggered grid. *Mon. Wea. Rev.*, **116**, 2069-2080.

Purser, R. J., and L. M. Leslie, 1991: An efficient interpolation procedure for high-order three-dimensional semi-Lagrangian models. *Mon. Wea. Rev.*, **119**, 2492-2498.

Purser, R. J., and L. M. Leslie, 1993: An efficient semi-Lagrangian scheme using third-order semi-implicit time integration and forward trajectories. *Mon. Wea. Rev.*, in press.

Staniforth, A., and J. Côté, 1991: Semi-Lagrangian integration schemes for atmospheric models-A review. *Mon. Wea. Rev.*, **119**, 2206-2223.

Sun, W.-Y., 1993: Comments on "A comparative study of numerical advection schemes featuring a one-step WKL algorithms". *Mon. Wea. Rev.*, **121**, 310-312.

Temperton, C., and A. Staniforth, 1987: An efficient two-time-level semi-Lagrangian semi-implicit integration scheme. *Quart. J. Roy. Meteor. Soc.*, **113**, 1025-1039.

Tremback, C. J., J. Powell, W. R. Cotton, and R. A. Pielke, 1987: The forward-in-time upstream advection scheme: Extension to higher orders. *Mon. Wea. Rev.*, **115**, 540-555.

Zalesak, S. T., 1979: Fully multidimensional flux-corrected transport algorithms for fluids. *J. Comput. Phys.*, **31**, 335-362.